Effect of shear wall location in rigid frame on earthquake response of roof structure

Koichiro Ishikawa[†], Yoshizo Kawasaki[‡] and Kengo Tagawa[‡†]

Department of Architecture and Civil Engineering, Fukui University, Fukui-shi 910-8507, Japan

Abstract. The purpose of this study is to investigate the effect of the shear wall location in rigid frames on the dynamic behavior of a roof structure due to vertical and horizontal earthquake motions. The study deals with a gabled long span beam supported by two story rigid frames with shear walls. The earthquake response analysis is carried out to study the responses of the roof: vibration mode, natural period, bending moment and horizontal shear force of the bearings. The study results in the following conclusions: First, a large horizontal stiffness difference between the side frames is caused by the shear wall location, which results in a large vertical vibration of the roof and a large shear force at the side bearings. Second, in this case, the seismic design method for ordinary buildings is not useful in determining the distribution of the static equivalent loads for the seismic design of this kind of long span structures.

Key words: long span structure; earthquake response; horizontal rigidity; interaction of long span beam and bearing structure.

1. Introduction

The paper is concerned with the seismic design of a long span roof structure considering the interaction of lightweight roof structures and their supporting heavyweight bearing structures such as RC rigid frames with shear walls. The static seismic design method for ordinary buildings may be frequently used in design practice for the design instead of the dynamic analysis (AIJ 1993, SEAOC 1996, Eurocode No.8 1998). In the case of the long span structures, the effect of the distribution of horizontal stiffness of the bearing structures on the maximum dynamic responses, such as the maximum acceleration, velocity and displacement should be studied to estimate the static equivalent load corresponding to the interaction (Eppo *et al*. 1993).

The present paper focuses on the earthquake response of a gabled roof structure supported by two story rigid frames with shear walls. The shear walls are not symmetrically placed within the rigid frames. Since it is difficult to estimate the static equivalent load for the seismic design of a long span roof structure with a pin support, dynamic analysis may be needed to obtain the seismic load distribution (Rosenblueth 1980, Blandford 1997).

The purpose of this study is to investigate difference between the dynamic response due to vertical and horizontal earthquake motions and static responses obtained for the structure subjected

† Associate Professor
‡ Auditor
‡† Professor

to the horizontal static seismic load using the seismic design method for ordinary buildings (AIJ 1993). The results will be shown to be useful for predicting the seismic load distribution and understanding the significant seismic design parameters.

2. Analyzed models

The study deals with long span gabled beam responses due to earthquake motion, which is supported by rigid frames with shear walls. The unbalanced location of shear walls may cause structural horizontal rigidity differences.

Three frame models are considered in the studies, which are classified as Models W, G and F. Model W is based on the structure in Fig. 1. The vibration shape and the response moment of the beam are affected by the horizontal rigidity difference between the two walls, as shown in Fig. 6. Models G and F are shown in Figs. 9(a) and (b), respectively. The effect of axial rigidity of the beam and the rigidity difference of the bearings on the horizontal shear reaction at the bearings is investigated using the two models.
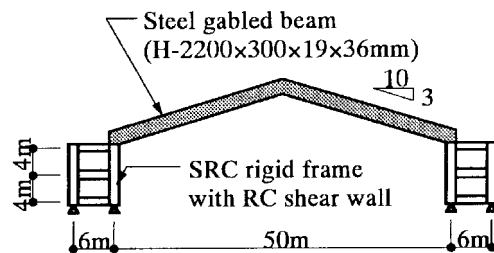
Fig. 1 Long span gabled roof structure supported by rigid frames with shear walls
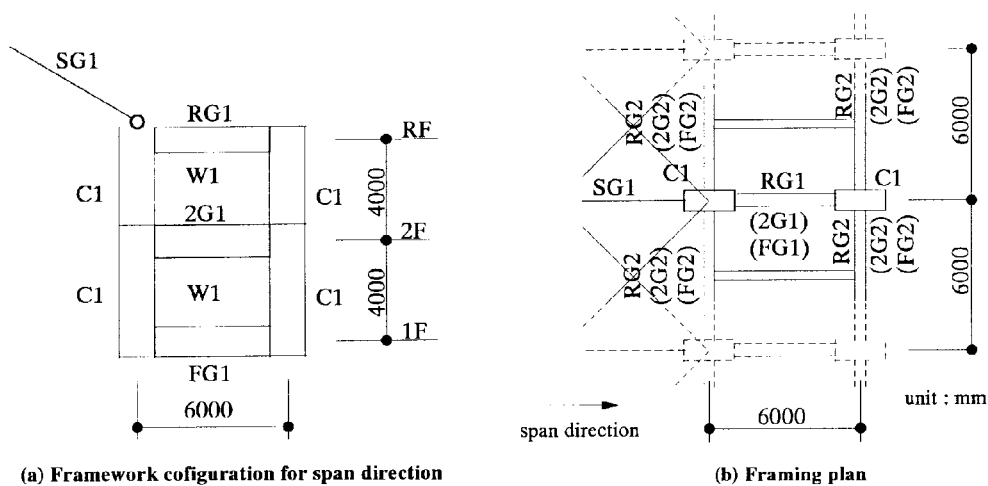
(a) Framework cofiguration for span direction   (b) Framing plan

Fig. 2 Framework of analyzed models (Member sections of the marks in figure are described in Table 1)

Table 1 Members section (See Fig. 2)

Mark	Section	
SG1	H-2200 × 300 × 18 × 36	
C1	*B*=800 mm	*D*=1400 mm
RG1	500	1000
2G1	500	1300
FG1	500	1200
RG2	400	700
2G2	400	800
FG2	500	1000
W1	*t*=250 mm	

2.1 Model W (Long span gabled roof structure supported by rigid frames with shear walls)

The structures are composed of H-section steel beams (H-2200 × 300 × 19 × 36 mm) supported on the two bearings at the top of the RC rigid frames with the shear walls, as shown in Figs. 1 and 2
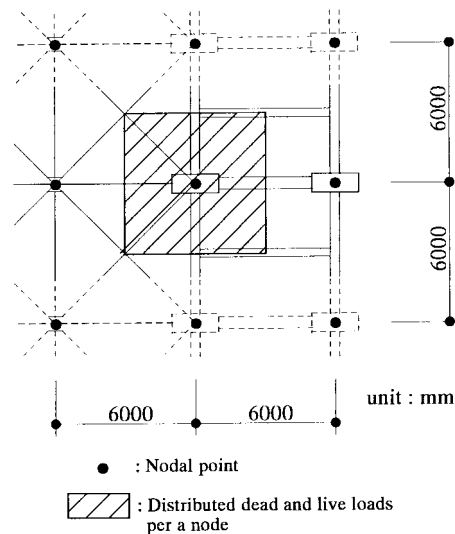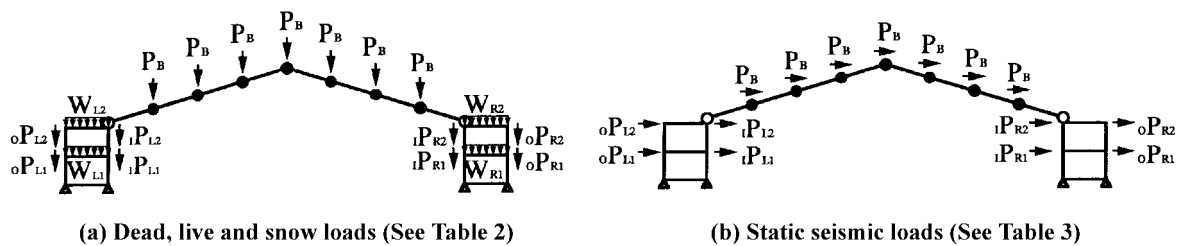

Fig. 3 Nodal concentrated load *P* equivalent to distributed dead and live loads

(a) Dead, live and snow loads (See Table 2)   **(b) Static seismic loads (See Table 3)**

Fig. 4 Applied static loads for structural design

Table 2 Dead, live and snow loads

Model No.	P_B (N)	$_oP_{L2}$ (N)	$_iP_{L2}$ (N)	$_oP_{L1}$ (N)	$_iP_{L1}$ (N)	$_oP_{R2}$ (N)	$_iP_{R2}$ (N)	$_oP_{R1}$ (N)	$_iP_{R1}$ (N)	W_{L2} (N/m)	W_{L1} (N/m)	W_{R2} (N/m)	W_{R1} (N/m)
1	214718	221774	329084	305270	305270	221774	329084	305270	305270	37632	34594	37632	44100
2	214718	221774	329084	305270	305270	221774	329084	305270	305270	37632	34594	47628	44590
3	214718	221774	329084	305270	305270	221774	329084	305270	305270	37632	34594	47628	54194
4	214718	221774	329084	305270	305270	221774	329084	305270	305270	37632	44100	47628	44590
5	214718	221774	329084	305270	305270	221774	329084	305270	305270	37632	44100	47628	54194
6	214718	221774	329084	305270	305270	221774	329084	305270	305270	47628	44590	47628	54194

Table 3 Static seismic loads

| Model No.	P_B (N)	$_oP_{L2}$ (N)	$_iP_{L2}$ (N)	$_oP_{L1}$ (N)	$_iP_{L1}$ (N)	$_oP_{R2}$ (N)	$_iP_{R2}$ (N)	$_oP_{R1}$ (N)	$_iP_{R1}$ (N)
1	33418	70266	87024	52822	52822	70266	87024	55860	55860
2	33418	69972	86632	52430	52430	75558	92218	55664	55664
3	33418	70266	87024	52822	52822	75852	92610	59094	59094
4	33418	70266	87024	55860	55860	75852	92610	56056	56056
5	33418	70560	87318	55860	55860	76244	93002	59094	59094
6	33418	75852	92610	56056	56056	75852	92610	59094	59094
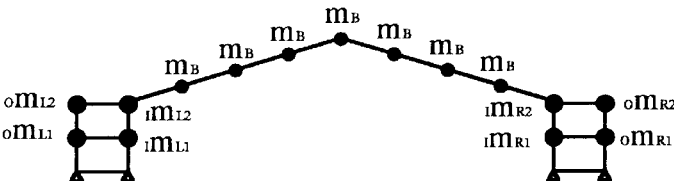
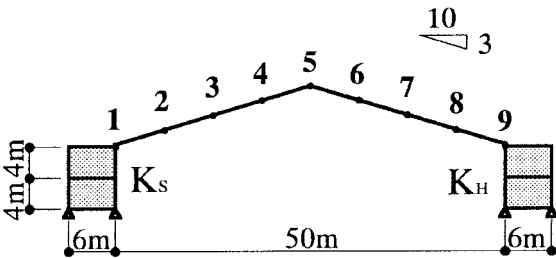Fig. 5 Mass distribution for dynamic analysis (See Table 4)

Fig. 6 Model W (Node number of beam and stiffness rigidities K_S of left side frame and K_H of right side frame)

with the section properties for the member of Fig. 2 given in Table 1. The Young's modulus of the steel and RC is taken to be 210 Gpa and 21 Gpa, respectively.

The structure has the following global geometry: the span of both frames is 6 m, the height of the 1st and 2nd stories is 4 m, the span of the center of the structure is 50 m and the slope of the roof is 3/10, as shown in Fig. 1.

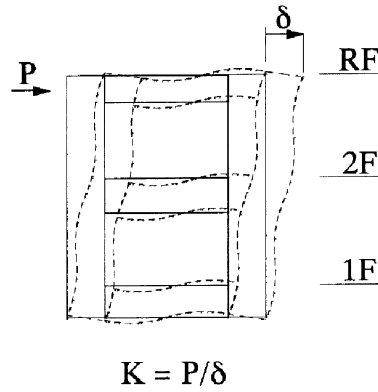The beam node numbers and structural geometry are shown in Fig. 6.

$$K = P/\delta$$

Fig. 7 Horizontal stiffness K at roof floor level of RC rigid frame

Table 4 Lumped masses (See Fig. 5)

Model No.	m_B (kg)	$_O m_{L2}$ (kg)	$_I m_{L2}$ (kg)	$_O m_{L1}$ (kg)	$_I m_{L1}$ (kg)	$_O m_{R2}$ (kg)	$_I m_{R2}$ (kg)	$_O m_{R1}$ (kg)	$_I m_{R1}$ (kg)
W1	14040	29510	36530	38800	38800	29510	36530	41030	41030
W2	14040	29510	36530	38800	38800	31870	38890	41160	41160
W3	14040	29510	36530	38800	38800	31870	38890	43390	43390
W4	14040	29510	36530	41030	41030	31870	38890	41160	41160
W5	14040	29510	36530	41030	41030	31870	38890	43390	43390
W6	14040	31870	38890	41160	41160	31870	38890	43390	43390

(a) Model W1   Shear wall   (d) Model W4

(b) Model W2   (e) Model W5
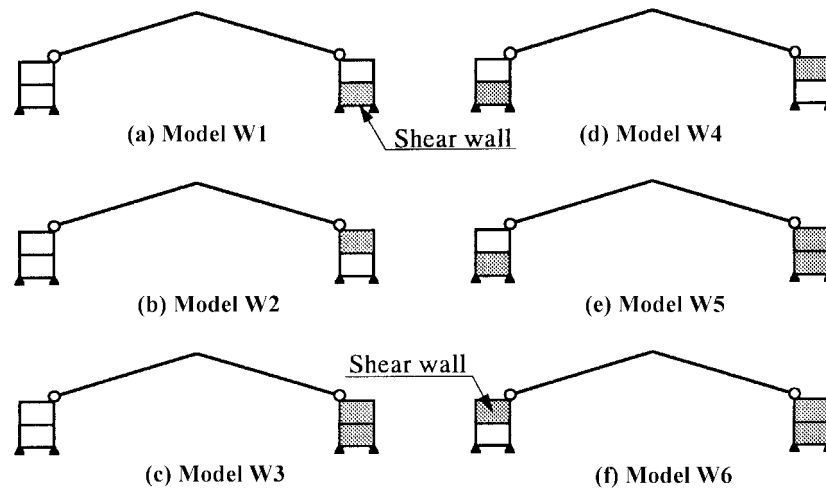
Shear wall

(c) Model W3   (f) Model W6

Fig. 8 Analyzed models (Model W) (Shear walls are located at hatched rectangles)

2.1.1 Structural design load

The characteristics of the members are determined by the structural design using the static analysis of the structure due to the design loads such as the dead, live, snow and seismic loads in

Table 5 Stiffness rigidities K_S and K_H of structures and ratio r_{HS} ($=K_H/K_S$) (See Fig. 6)

Group	Model No.	K_S (10^5 kN/m)	K_H (10^5 kN/m)	r_{HS}
A	1	1.05	4.05	3.86
	2	1.05	4.30	4.09
	3	1.05	10.54	10.03
B	4	4.05	4.30	1.06
	5	4.05	10.54	2.60
	6	4.30	10.54	2.45

(a) Model G (Gabled beam) (b) Model F (Flat beam)
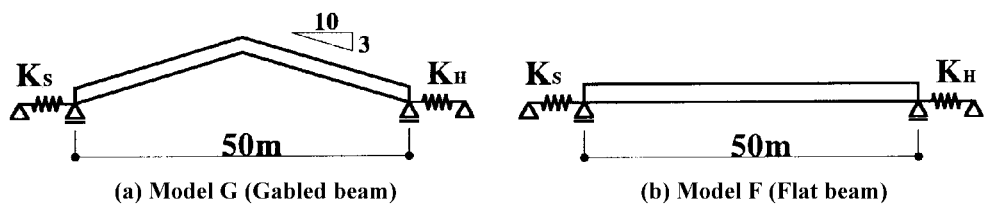
Fig. 9 Gabled and flat beams with different horizontal stiffness rigidity of bearing structures at both side bearings
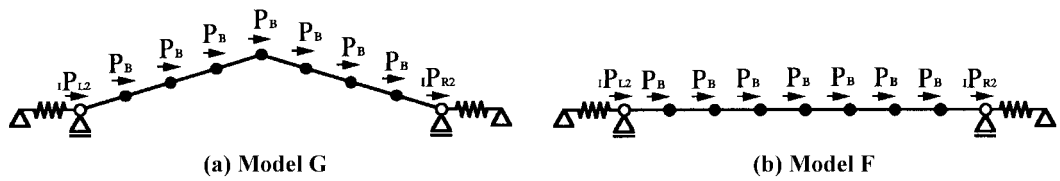

(a) Model G (b) Model F

Fig. 10 Static seismic design loads

Figs. 2, 3 and 4. The numerical values of the loads are given in Tables 2 and 3.

2.1.2 Models W1-W6

Based on the global configuration, the analyzed models (Models W1-W6) are shown in Fig. 8. The dynamic behavior of the six long span structures varying the location of the shear wall is investigated to see the effect of the horizontal stiffness distribution of the bearing structures. It is noticed that the location of the shear walls of the models is different in order to study the effect of the unbalanced horizontal rigidity of the side frames.

The horizontal rigidities of K_S (soft rigidity) and K_H (hard rigidity) of the side frames are shown in Table 5. And the ratio r_{HS} of K_H divided by K_S is defined to measure the degree of unbalanced horizontal rigidity between the side frames. It is seen that the Models W1 to W3 result in the large differences in the lateral rigidities in comparison with Models W4 to W6.

Table 6 Static seismic design loads (See Fig. 9)

Mark	Load (N)
P_B	33418
P_L, P_R	218638

Table 7 Mass (See Fig. 10)

Mark	Mass (kg)
m_B	14040
m_L, m_R	110×10^6

2.2 Models G and F

The structure in Fig. 1 may be equivalent to the model in Fig. 9(a). The static seismic design load and mass are shown in Fig. 10, with the respective values given in Tables 6 and 7. The study also deals with the flat beam in Fig. 9(b) in order to investigate the effect of axial rigidity of the beam on the shear force at the bearings.

The twenty-one gabled beam models and the twenty-one flat beam models are shown in Table 8 corresponding to the stiffness rigidities K_S and K_H of the bearing structures.

The maximum reaction of the horizontal shear force at the side bearings of the gabled beam is investigated using the dynamic analysis.
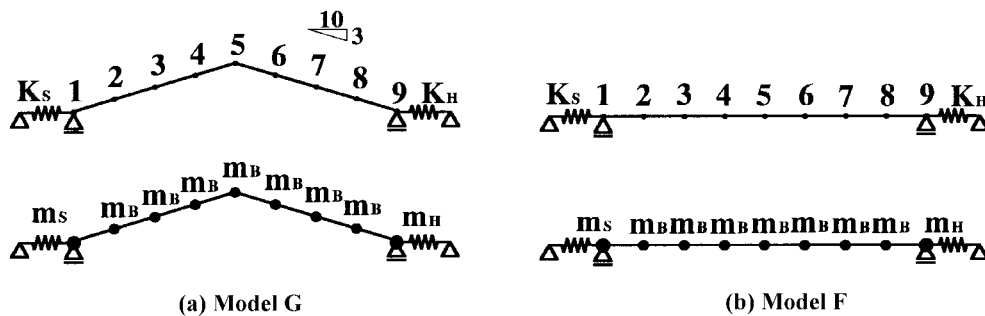
(a) Model G   **(b) Model F**

Fig. 11 Node number and mass distribution

Model 1   **Model 2**   **Model 3**   **Model 4**   **Model 5**   **Model 6**
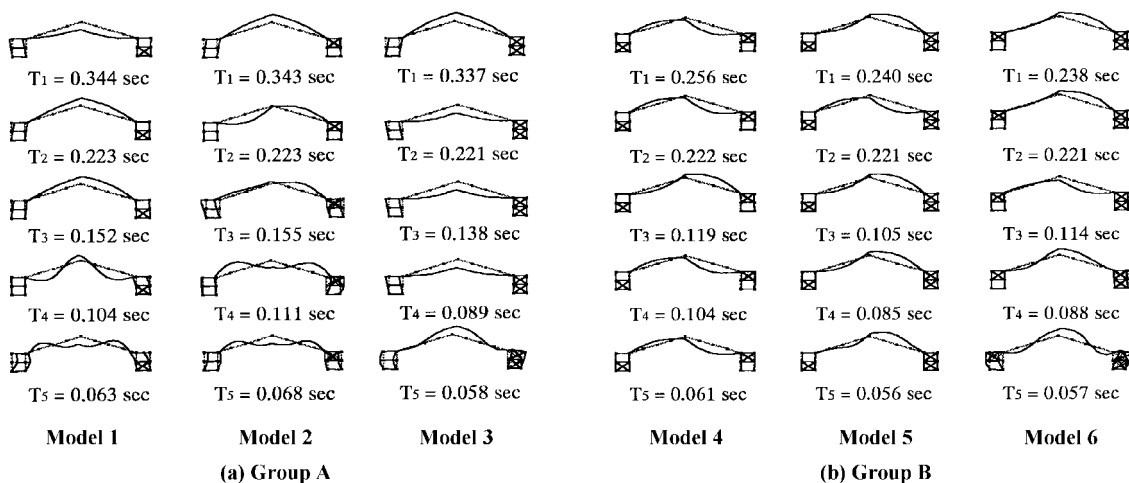
(a) Group A   **(b) Group B**

Fig. 12 Natural periods of models W1 to W6 and corresponding vibration mode shapes

Table 8 Stiffness rigidities K_H (hard rigidty) and K_S (soft rigidty) of gabled and flat beams and r_{HS} (=K_H/K_S)

Model No.	K_H (10^5 kN/m)	K_S (10^5 kN/m)	r_{HS}	Model No.	K_H (10^5 kN/m)	K_S (10^5 kN/m)	r_{HS}
G1	1.00	1.00	1.00	F1	1.00	1.00	1.00
G2	1.20	1.00	1.20	F2	1.20	1.00	1.20
G3	1.40	1.00	1.40	F3	1.40	1.00	1.40
G4	1.60	1.00	1.60	F4	1.60	1.00	1.60
G5	1.80	1.00	1.80	F5	1.80	1.00	1.80
G6	2.00	1.00	2.00	F6	2.00	1.00	2.00
G7	2.20	1.00	2.20	F7	2.20	1.00	2.20
G8	2.40	1.00	2.40	F8	2.40	1.00	2.40
G9	2.60	1.00	2.60	F9	2.60	1.00	2.60
G10	2.80	1.00	2.80	F10	2.80	1.00	2.80
G11	3.00	1.00	3.00	F11	3.00	1.00	3.00
G12	3.20	1.00	3.20	F12	3.20	1.00	3.20
G13	3.40	1.00	3.40	F13	3.40	1.00	3.40
G14	3.60	1.00	3.60	F14	3.60	1.00	3.60
G15	3.80	1.00	3.80	F15	3.80	1.00	3.80
G16	4.00	1.00	4.00	F16	4.00	1.00	4.00
G17	4.20	1.00	4.20	F17	4.20	1.00	4.20
G18	4.40	1.00	4.40	F18	4.40	1.00	4.40
G19	4.60	1.00	4.60	F19	4.60	1.00	4.60
G20	4.80	1.00	4.80	F20	4.80	1.00	4.80
G21	5.00	1.00	5.00	F21	5.00	1.00	5.00

3. Vibration mode shape and natural period of Model W

The eigen value analysis of Model W is carried out. The vibration mode shapes and the natural periods for the 1st to 5th modes are shown in Fig. 12. It is seen that the vertical movement of the beam appears in the 1st mode shape of Models W1, W2 and W3 (Group A). On the other hand, both horizontal and vertical movements of the beams can be seen in the first mode shape of Models W4, W5 and W6 (Group B). The first natural period T_1 of Models W1 to W3 results in almost the same value of 0.34 sec. The mean T_1 value of Models W4 to W6 is 0.25 sec. We can see a large value difference in the first mode shape and the corresponding natural period between Groups A and B.

4. Earthquake response of beam and bearing

The lumped masses for the eigen value analysis and the earthquake response analysis are distributed at the nodes, as shown in Fig. 5 and the mass values are given in Table 4. In this study, the distribution of the maximum response of the elastic time-history dynamic analysis is compared with the result of the static analysis subjected to the horizontal seismic load.

4.1 Response moment at beam of Model W

The dynamic analysis of all the six models is carried out to investigate the earthquake response of

the beam. Three input waves are used in the analysis. The peak acceleration and the component of the input wave direction are the following: Kobe NS (Peak acceleration=200 cm/sec^2) and UD (100 cm/sec^2), El-Centro NS (200 cm/sec^2) and UD (100 cm/sec^2), and Osaka NS (200 cm/sec^2) and UD (100 cm/sec^2), where NS signifies north-south direction and UD means vertical direction.

The mean maximum bending moment response with respect to the three input waves at the node points (see Fig. 6) of the beams are shown in Fig. 13.

The distinct moment distribution between Groups A and B is seen in Fig. 13. In Group A (Models W1 to W3), large rigidity difference between the side frames brings about the vertical vibration of the beam due to the horizontal input wave. This is the reason why the moment around the middle of the beam results in the large values and a little difference of the response of the two cases between the only horizontal wave and both the horizontal and vertical input waves. On the other hand, the beams of Group B (Models W4 to W6) due to the three input wave cases bring about moments that are less than those of Group A. Vertical vibration of the beams is not induced by rigidity differences of the frames in Group B.
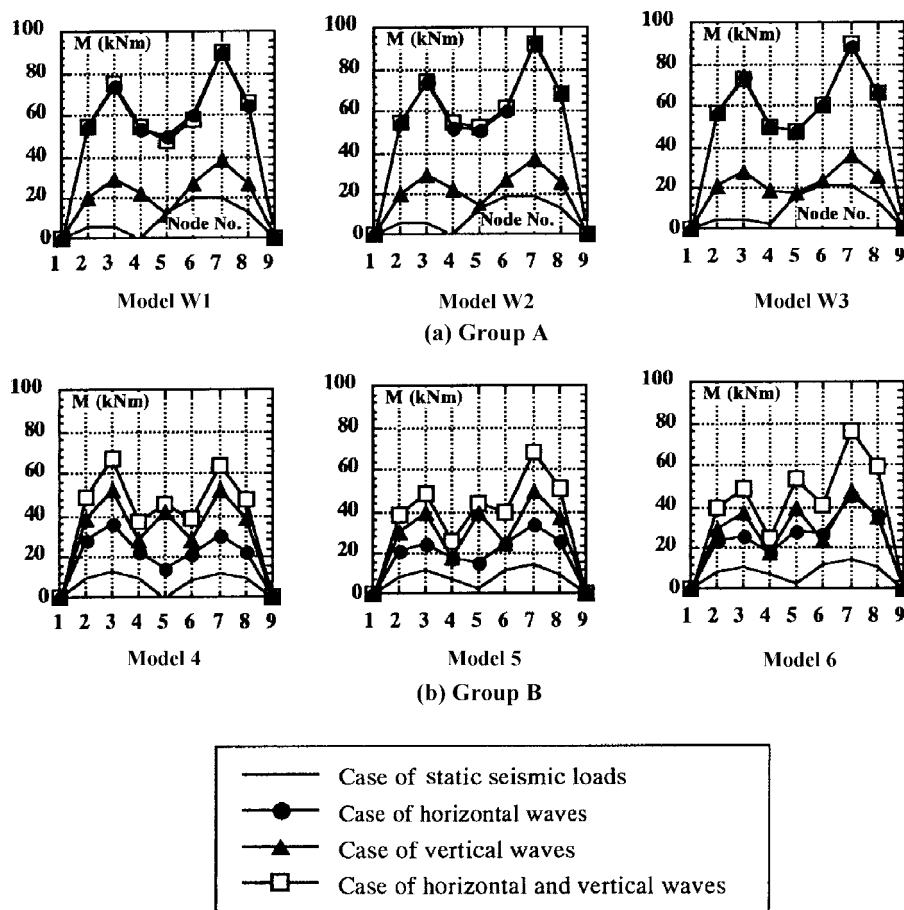

Fig. 13 Mean value of maximum response bending beam moments (M) of Model W due to three different input waves

The difference of the moment of the beam between the dynamic behavior due to the horizontal earthquake motion and the static behavior subjected to the seismic loads is investigated to evaluate the distribution of the seismic load for the seismic design of this kind of long span structures. It is seen that the seismic load needs to be modified with regard to the distribution corresponding to the ratio r_{HS}. Furthermore, it is noticed that large difference between static and dynamic responses appears in the left side of the beam supported the soft rigidity bearing, as shown in Group A.

In the case of Group B, the static response distribution due to the seismic design load shows agreement with the dynamic response, though the magnitudes are much smaller.

4.2 Response shear force at bearings of Models G and F

The study also focuses on the shear force of the bearing induced by the different horizontal rigidity of the bearing structure using Models G and F.

Fig. 14(a) shows the relationship between the ratio r_{HS} ($=K_H/K_S$) and mean values of the maximum response shear coefficient (shear force/($\Sigma m_B + m_S + m_H$), see Fig. 11) at the bearings with respect to
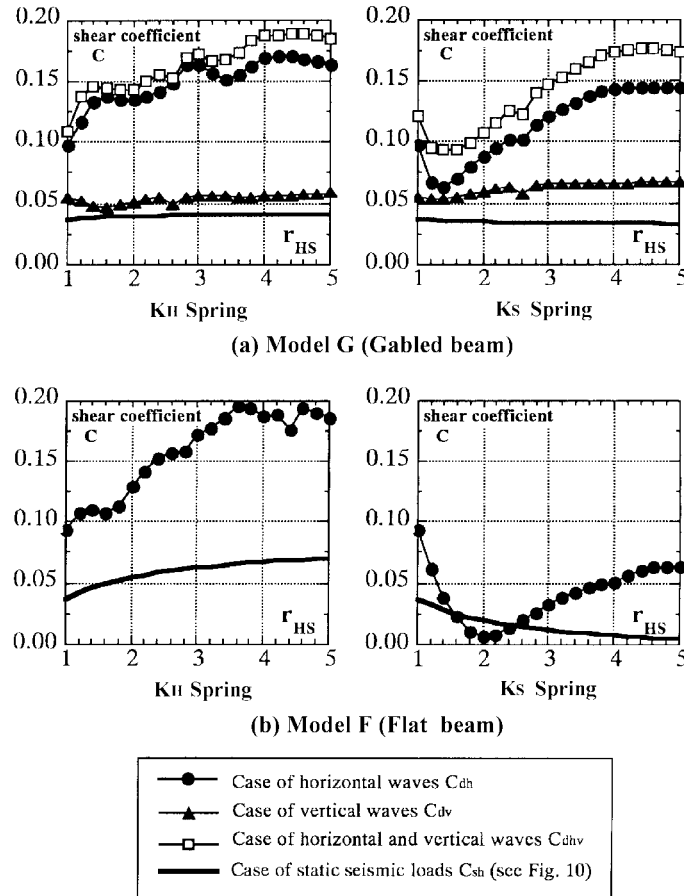

Fig. 14 Relationship between r_{HS} ($=K_H/K_S$) and shear coefficient C at left and right springs

the three waves used in the study.

In the case of the gabled beam, the reaction under the static load results in a shear coefficient around 0.03 for all values r_{HS}. In the cases of the horizontal wave and both horizontal and vertical waves, a large difference between K_S and K_H results in a much greater variation of the shear coefficient at the soft rigidity bearing. The thrust of the gabled beam due to vertical motion may bring about the difference.

In the case of the flat beam, the spring reaction difference between the static and dynamic responses exhibits a somewhat greater variability with r_{HS} as compared to the gabled beam results. This is because of the axial rigidity difference of the beams.

Fig. 15 shows the computed relationship between r_{HS} and the ratio of the dynamic reaction divided by the static results of Fig. 14. From Fig. 15(b), a large difference between the soft and hard bearings appears in the range of r_{HS} greater than the value around 3. Accordingly, it may be needed for engineers to carry out the dynamic analysis for predicting precisely the soft side reaction in the case of the beam with the hard axial rigidity.
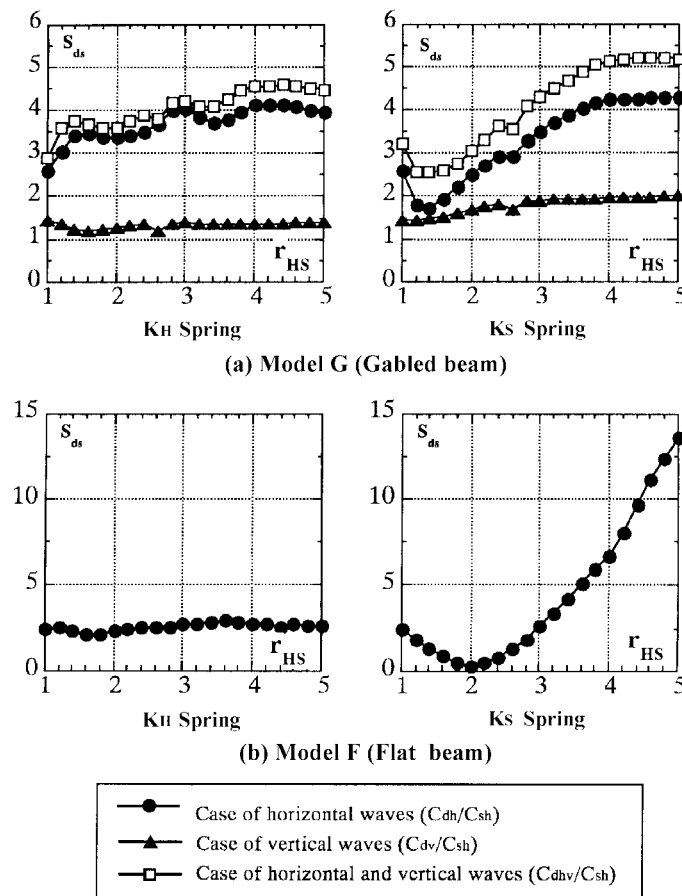

Fig. 15 Relationship between r_{HS} and ratio of dynamic response shear coefficient C_d and static response shear coefficient C_s ($S_{ds}=C_d/C_s$)

5. Conclusions

The study has carried out the earthquake response analysis of gabled and flat beams supported by bearing structures. Their beam models were supported by bearings with the different horizontal rigidities and were subjected to vertical, horizontal and both horizontal and vertical input waves. The study has shown the effect of the rigidity difference of the berings on the response moment of the beams and the response shear force of the bearings.

The conclusions of the study are:

(1) In the case of a large horizontal unbalanced rigidity between the side frames, a horizontal ground wave brings about a large vertical vibration of the beam when compared to beam with more nearly equal horizontal rigidities.

(2) In the case of large differences in the side bearing rigidities, it may be difficult to estimate the soft bearing shear force using static seismic loads and static analysis. It is noticed that hard axial rigidity beams, such as a flat beam, affect the response shear force at the soft bearing.

References

Blandford, G.E. (1997), "Review of progressive failure analyses for truss structures", *J. of Struct. Eng.*, **123**(2), 122-129.

Eppo, A.S.K., and Karamanos, S.A. (1993), "Seismic design of double layer space grids and their supports", Space Structures 4, *Proc. of the Fourth Int. Conf. of Space Struct.*, Park, G.A.R. ed, 1, Thomas Telford, 476-484.

Eurocode No.8 (1998), "Design of structures in seismic regions", European Committee for Standardization (CEN) Standards.

Rosenblueth, E. (1980), *Design of Earthquake Resistant Structures*, Pentech Press.

SEAOC (1996), "Recommended lateral force requirements and comenmentary", *Structural Engineers Association of California's (SEAOC) Recommendations and Commentary for Earthquake-Risistant Design of Structures*, SEAOC Blue Book, SESP 96.

The Architectural Institute of Japan (1993), "Earthquake motion and ground conditions", AIJ edn., Japan, 471-483.

The Architectural Institute of Japan (1997), "Report on the Hanshin-Awaji earthquake disaster", *Structural Damage to Shell and Spatial Structures*, AIJ edn., Building Series, Japan, **3**, 219-346.

Yigang, Z., and Lan, T.T. (1985), "A practical method of space frames under vertical earthquake", *J. of Building Struct.*, 5.